

Superhumps and their Amplitudes

J. S m a k

N. Copernicus Astronomical Center, Polish Academy of Sciences,
Bartycka 18, 00-716 Warsaw, Poland
e-mail: jis@camk.edu.pl

Received

ABSTRACT

Superhump amplitudes observed in dwarf novae during their superoutbursts depend on orbital inclination: the maximum amplitudes in systems with low inclinations are $A_o \approx 0.25$ mag., while at higher inclinations they increase from $A_o \sim 0.3$ to $A_o \sim 0.6$ mag.

The mean maximum superhump amplitudes normalized to the average luminosity of the disk are: $\langle A_n \rangle = 0.34 \pm 0.02$ in low inclination systems and only $\langle A_n \rangle = 0.17 \pm 0.01$ in high inclination systems. This shows that at high inclinations the superhump light source is *partly* obscured by the disk edge and implies that it is located close to the disk surface but extends sufficiently high above that surface to avoid full obscuration. Superhump amplitudes in high inclination systems show modulation with beat phase (ϕ_b), interpreted as being due to azimuth-dependent obscuration effects in a non-axisymmetric disk. In addition they show modulation with $2\phi_b$ which implies that the orientation of the superhump light source is correlated with the direction of the stream.

The dependence of superhump amplitudes on orbital inclination and their modulation with beat phase eliminate the tidal-resonance model for superhumps. Instead they support an alternative interpretation of superhumps as being due to periodically modulated dissipation of the kinetic energy of the stream.

Superhump amplitudes in permanent superhumpers are $\langle A \rangle = 0.12$, i.e. much smaller than the maximum amplitudes observed during superoutbursts.

Key words: *accretion, accretion disks – binaries: cataclysmic variables, stars: dwarf novae*

1. Introduction

Superhumps were discovered by Vogt (1974) and Warner (1975) during the December 1972 superoutburst of VW Hyi. It is now well established that they are present in all dwarf novae of the SU UMa type during their superoutbursts (see Warner 1995, Hellier 2001). Their periods are slightly longer than the orbital periods and usually show complex variations (cf. Kato et al. 2009). Superhumps are also present in the so-called permanent superhumpers – the nova-like cataclysmic binaries with stationary accretion (cf. Patterson 1999) as well as in some dwarf novae at quiescence (Still et al. 2010 and references therein).

Any periodic phenomenon is characterized by two parameters: the period and the amplitude. In the case of superhumps, however, most authors concentrate primarily or even exclusively on the superhump periods, treating their amplitudes as less important. Of course, there are papers (e.g. Warner and O'Donoghue 1988, Olech et al. 2003) which present full description of superhumps, including their individual light curves, but – regretfully – they belong to minority. A typical paper in this field (see, for example, Kato et al. 2009) contains "journals of observations" (which are meaningless), tables containing moments of superhump maxima (but not their amplitudes!), figures showing the (O-C) diagrams and – not always – only the *mean* superhump light curves without any information on their variations.

As a result of this attitude our knowledge about superhump amplitudes has been, until now, limited to the few following conclusions:

(1) Superhumps first appear around superoutburst maximum (or shortly earlier; see Semeniuk 1980) and reach their highest amplitude either at maximum or 1-2 days later.

(2) Superhump amplitudes decrease during superoutburst; this effect, however, has been well documented only for relatively few cases (e.g. Warner and O'Donoghue 1988, Fig.5; Patterson et al. 2000b, Fig.10; Rutkowski et al. 2007, Fig.4).

(3) According to Warner (1995, p.194): "At their full development the superhumps have a range of 0.3-0.4 mag. and are equally prominent in all SU UMa stars *independent of inclination*".

(4) According to Warner (1985, p.372): "There is no strong modulation of the superhump profile at the beat period."

As it will turn out (see Section 3) the last two statements are not true.

The aim of the present paper is to improve the situation by presenting new results concerning superhump amplitudes based on representative samples of dwarf novae at their superoutbursts and of permanent superhumpers.

2. Definitions and Formulae

2.1. The Amplitudes of Superhumps

In what follows we will discuss the *full* amplitudes of superhumps. With this definition the superhump amplitude – in intensity units – is given by

$$a = \frac{\ell_{max} - \ell_{min}}{\ell_{min}} = \frac{\ell_{sh}}{\ell_d}, \quad (1)$$

where $\ell_d = \ell_{min}$ is the luminosity of the disk, and ℓ_{sh} is the luminosity of the superhump at its maximum. It is more common, however, to express superhump amplitudes in magnitudes:

$$A(\text{mag}) = 2.5 \log (1 + a) . \quad (2)$$

Note that in both cases the superhump amplitude is defined with respect to the luminosity of the disk.

2.2. *The Normalized Superhump Amplitudes*

The observed luminosity of the disk depends on inclination. At low inclinations this dependence can be described with a simple formula applicable to a flat disk with limb darkening $u = 0.6$:

$$\ell_d(i) = \langle \ell_d \rangle (1 + 1.5 \cos i) \cos i . \quad (3)$$

At inclinations higher than $i \sim 70^\circ$, however, it is necessary to include contributions from the disk edge and – at $i > 80^\circ$ – effects of self-occlusion. For the purpose of the present discussion a sequence of steady-state disk models was calculated, using model parameters of Z Cha and $\dot{M} = 3 \times 10^{17}$ g/s. Results can be represented by an approximate formula replacing Eq.(3) for $i > 60^\circ$:

$$\ell_d(i) = \langle \ell_d \rangle (3.414 - 0.05374 i + 0.00020 i^2) . \quad (4)$$

The superhump amplitude normalized to $\langle \ell_d \rangle$ can then be computed from

$$A_n(\text{mag}) = 2.5 \log \left[1 + \left(10^{0.4A} - 1 \right) \frac{\ell_d(i)}{\langle \ell_d \rangle} \right] . \quad (5)$$

2.3. *The Beat Phases*

The beat phase is related to the orbital and superhump phases by

$$\phi_b = \phi_{orb} - \phi_{sh} , \quad (6)$$

and at the superhump maximum when $\phi_{sh} = 0$ we simply have: $\phi_b = \phi_{orb}$.

3. Superhump Amplitudes in Dwarf Novae at their Superoutbursts

3.1. Data and their Analysis

A search through the literature resulted in a sample of 26 dwarf novae (Table 1) with data on their superhump amplitudes suitable for our discussion. It includes 11 eclipsing systems with well determined orbital inclinations ($i \geq 79^\circ$) taken from the Catalogue by Ritter and Kolb (2003) and 15 non-eclipsing systems with unknown, much lower inclinations.

Using earlier evidence (see Introduction) we assume that variations of the superhump amplitude with time during superoutburst can be represented by

$$A = A_o + \frac{dA}{dt} \Delta t, \quad (7)$$

where $dA/dt < 0$ and $\Delta t = 0$ corresponds to the maximum amplitude A_o .

The data on superhump amplitudes for objects listed in Table 1 were analysed using Eq.(7) and the resulting values of A_o and dA/dt are listed in columns 3 and 4 of this table. As could be expected they are tightly correlated

$$\frac{dA}{dt} = C A_o. \quad (8)$$

where $C = 0.063 \pm 0.005$.

At this point we can comment on the uncertainty of the values of A_o resulting from the fact that the moments $\Delta t = 0$ are not always precisely known. An uncertainty of ± 1 day in the zero point of Δt translates into an additional uncertainty of A_o as $\pm dA/dt = \pm 0.063A_o$ which is comparable or larger than formal errors listed in Table 1. Fortunately this additional uncertainty does not affect our main results.

The procedure described above could not be applied to four high inclination systems (V2051 Ori, OU Vir, J1524+2209, and J1702+3229) for which only the *mean* light curves were available. Their maximum superhump amplitudes A_o were estimated from the mean amplitudes $\langle A \rangle$ corresponding to the mean $\langle \Delta t \rangle$

Table 1
Amplitudes of Superhumps
Dwarf Novae at Superoutbursts

Star	<i>i</i>	A_o (mag)	dA/dt (mag/d)	Data
V1141 Aql		0.33 ± 0.02	-0.034 ± 0.006	1
V877 Ara		0.26 ± 0.01	-0.019 ± 0.002	2
TT Boo		0.24 ± 0.02	-0.008 ± 0.002	3
OY Car	83.3	0.51 ± 0.03	-0.041 ± 0.004	4,5
V485 Cen		0.22 ± 0.01	-0.021 ± 0.002	6
Z Cha	80.2	0.49 ± 0.03	-0.046 ± 0.006	7
EG Cnc		0.22 ± 0.02	-0.012 ± 0.002	8
V503 Cyg		0.17 ± 0.01	-0.005 ± 0.003	9
IX Dra		0.16 ± 0.03	-0.014 ± 0.007	10
XZ Eri	80.2	0.29 ± 0.05	-0.008 ± 0.008	11,12
V660 Her		0.32 ± 0.02	-0.020 ± 0.003	13
VW Hyi		0.30 ± 0.01	-0.019 ± 0.002	14
V419 Lyr		0.30 ± 0.01	-0.015 ± 0.002	15
V1159 Ori		0.20 ± 0.03	-0.030 ± 0.008	16
V2051 Ori	83.0	0.50 ± 0.10		17
SW UMa		0.25 ± 0.01	-0.023 ± 0.002	18
CY UMa		0.28 ± 0.02	-0.021 ± 0.005	19
DI UMa		0.21 ± 0.02	-0.019 ± 0.003	20
DV UMa	84.0	0.61 ± 0.04	-0.032 ± 0.004	21
IY UMa	86.8	0.69 ± 0.08	-0.036 ± 0.008	22
KS UMa		0.21 ± 0.03	-0.009 ± 0.005	23
OU Vir	79.2	0.34 ± 0.10		24
J1227+5139	83.9	0.51 ± 0.04	-0.028 ± 0.006	25
J1502+3334	88.9	0.53 ± 0.04	-0.018 ± 0.007	26
J1524+2209	82.8	0.30 ± 0.10		27
J1702+3229	82.4	0.60 ± 0.10		28,29

Data sources: (1) Olech (2003) Fig.3. (2) Kato et al. (2003) Fig.3. (3) Olech et al. (2004b) Fig.5. (4) Krzemiński and Vogt (1985) Fig.2b. (5) Schoembs(1986) Fig.2a. (6) Olech (1997) Figs 2 and 4. (7) Warner and O'Donoghue (1988) Table 3 and Fig.5. (8) Patterson et al. (1998) Table 1. (9) Harvey et al. (1995) Fig.7. (10) Olech et al. (2004a) Fig.10. (11) Uemura et al. (2004) Fig.4. (12) Patterson et al. (2005) Fig.2. (13) Olech et al. (2005) Fig.3. – continued on next page –

Table 1. Data sources – continued: (14) Haefner et al. (1979) Fig.7. (15) Rutkowski et al. (2007) Fig.4. (16) Patterson et al. (1995) Figs 4 and 5. (17) Kiyota and Kato (1998) Fig.2. (18) Soejima et al. (2009) Figs 2,9,14. (19) Harvey and Patterson (1995) Fig.2. (20) Rutkowski et al. (2009) Figs 4 and 7. (21) Patterson et al. (2000b) Fig.10. (22) Patterson et al. (2000a) Fig.2. (23) Olech et al. (2003) Fig.8. (24) Patterson et al. (2005) Fig.1. (25) Shears et al. (2008) Fig.3. (26) Shears et al. (2010) Fig.3. (27) Kato et al. (2009) Fig.191. (28) Boyd et al. (2006) Fig.8. (29) Kato et al. (2009) Fig.193.

using the following formula obtained by combining Eqs.(7) and (8)

$$A_o = \frac{\langle A \rangle}{1 - C \langle \Delta t \rangle}. \quad (9)$$

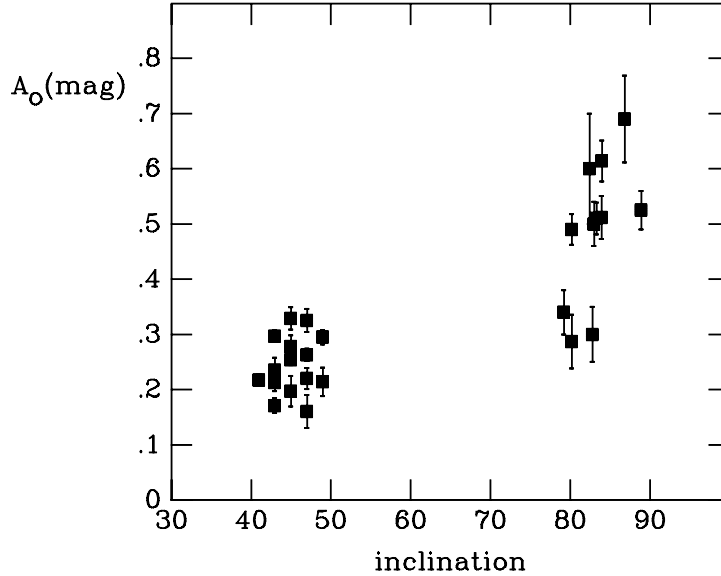


Fig. 1. Maximum superhump amplitudes A_o as a function of the orbital inclination. Non-eclipsing systems with unknown inclinations are plotted between $i = 40^\circ$ and 50° .

3.2. Maximum Superhump Amplitudes versus Orbital Inclination

Fig.1 shows the maximum superhump amplitudes A_o plotted against the orbital inclination. As we can see the values of A_o for low inclination system cluster around $A_o \approx 0.25$. Those for high inclination, eclipsing systems are – roughly – 2 times larger, show more scatter and appear to increase from $A_o \approx 0.3$ at $i \approx 80^\circ$ to about $A_o \sim 0.6$ at the highest inclinations.

This imposes important constraints on superhumps models and, in particular, eliminates all models which locate the superhump light source within the disk. As discussed above (Section 2) the superhump amplitude is defined with respect to the luminosity of the disk which depends strongly on inclination. Should the superhump source be located within the disk its luminosity would depend on inclination in the same way as the luminosity of the disk and the observed superhump amplitude would be independent of inclination.

Using Eq.(5) we now normalize the maximum superhump amplitudes A_o to the mean luminosity of the disk. For non-eclipsing systems, with inclinations which are generally lower than about 70° , assuming their random distribution we adopt: $\langle i \rangle = \langle i \sin i \rangle / \langle \sin i \rangle \approx 45^\circ$.

The resulting normalized amplitudes A_n are plotted against orbital inclination in Fig.2. Compared to Fig.1 the situation is now different. The superhump amplitudes of low inclination systems cluster around $\langle A_n \rangle = 0.34 \pm 0.02$ with *r.m.s.* dispersion of individual values $\sigma = \pm 0.07$. This value of A_n can then be considered as representative for superhumps observed during superoutbursts. The amplitudes of high inclination systems cluster around $\langle A_n \rangle = 0.17 \pm 0.01$, show scatter $\sigma = \pm 0.04$ which is much smaller than that in Fig.1, and do not show any dependence on inclination. The obvious interpretation is that the superhump source is located close to the disk surface but extends sufficiently high above that surface so that in systems with high inclinations it is *partly* obscured by the disk edge.

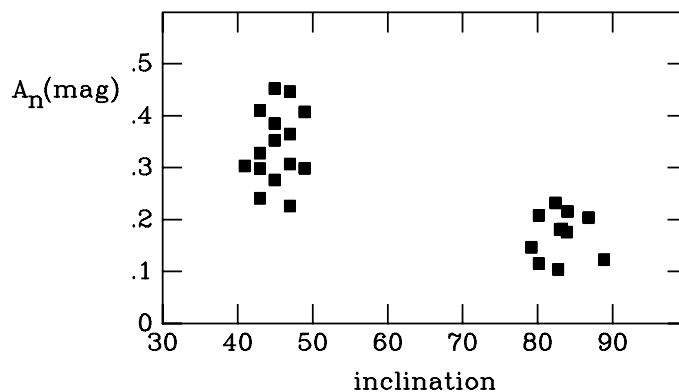


Fig. 2. Maximum superhump amplitudes normalized to the average disk luminosity as a function of the orbital inclination.

Not included in our discussion, so far, was U Gem. During its 1985 superoutburst it showed superhumps with amplitude $A \approx 0.3$ mag. (Smak and Waagen 2004). With $i = 69^\circ$ this places it in Fig.1 just between the low and high inclinations systems. Unlike in all other dwarf novae, however, the superhump amplitude of U Gem stayed constant throughout the entire superoutburst. There is no obvious

explanation of this peculiar behavior.

3.3. Dependence of Superhump Amplitudes on Beat Phase

The superhump amplitude can be modulated with beat phase due to various effects. Two such effects, suggested by earlier evidence, are considered here.

It was shown earlier (Smak 2009b) that in systems with the highest orbital inclinations ($i > 82^\circ$) their disk luminosity during superoutbursts is modulated with the beat period. This was interpreted as being due to a non-axisymmetric structure of the disk, involving the azimuthal dependence of the vertical thickness of its outer edge. At that time there were only three systems (OY Car, DV UMa and IY UMa) showing such modulation. Now we can strengthen our earlier conclusion by adding another deeply eclipsing system: J1227+5139. Using data from Shears et al. (2008) and reducing them in the same way as before (Smak 2009b, Section 2) we obtain the residual magnitudes which show clear dependence on the beat phase (Fig.3). The two parameters describing this dependence: the half-amplitude $A(\text{mag}) = 0.18 \pm 0.03$ and $\phi_b^{\text{max}} = 0.68 \pm 0.03$ are – within errors – identical with those obtained earlier for three other systems. Using now all four systems we get: $\langle A(\text{mag}) \rangle = 0.18 \pm 0.01$ and $\langle \phi_b^{\text{max}} \rangle = 0.65 \pm 0.02$. An obvious question is: do the amplitudes of superhumps show similar effect?

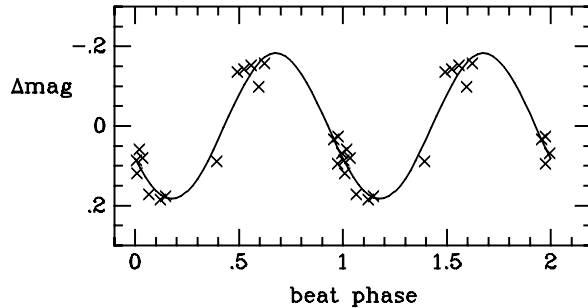


Fig. 3. Residual disk magnitudes for J1227+5139 are plotted against the beat phase. Solid line is the cosine curve with parameters given in the text.

Another effect, to be considered here, is suggested by earlier results concerning superhumps observed in U Gem during its December 1985 superoutburst. It was found (Smak 2006) that their amplitude was modulated with beat phase in the form of a *double* cosine wave. An obvious question is: do other dwarf novae show similar modulation?

To answer those questions we analyze data on superhumps for six high inclination and – for comparison – for four low inclination systems with sufficient

coverage in beat phases. The superhump amplitudes observed at Δt and at beat phase ϕ_b are represented with

$$A = A_o + \frac{dA}{dt} \Delta t + A_1 \cos (\phi_b - \phi_{b,1}^{max}) + A_2 \cos \left[2 (\phi_b - \phi_{b,2}^{max}) \right]. \quad (10)$$

The last term in this equation describes the "double- ϕ_b " modulation with two maxima at $\phi_{b,2}^{max}$ and $\phi_{b,2}^{max} + 0.5$ and two minima at $\phi_{b,2}^{max} \pm 0.25$.

The residuals ΔA , representing the "single- ϕ_b " and "double- ϕ_b " modulations, are calculated as

$$\Delta A = A - \left(A_o + \frac{dA}{dt} \Delta t \right). \quad (11)$$

Table 2
Amplitudes of Superhumps
Modulation with Beat Phase

Star	A_1	$\phi_{b,1}^{max}$	A_2	$\phi_{b,2}^{max}$
OY Car	0.02 ± 0.01	0.63 ± 0.13	0.04 ± 0.01	0.36 ± 0.12
Z Cha	0.04 ± 0.01	0.50 ± 0.05	0.07 ± 0.03	0.28 ± 0.03
DV UMa	0.08 ± 0.02	0.55 ± 0.03	0.07 ± 0.01	0.26 ± 0.02
IY UMa	0.11 ± 0.03	0.58 ± 0.05	0.01 ± 0.03	0.20 ± 0.11
J1227+5139	0.05 ± 0.02	0.99 ± 0.06	0.08 ± 0.03	0.25 ± 0.03
J1502+3334	0.06 ± 0.03	0.82 ± 0.16	0.09 ± 0.03	0.50 ± 0.02
TT Boo	0.02 ± 0.03		0.04 ± 0.03	
VW Hyi	0.01 ± 0.01		0.03 ± 0.01	
V419 Lyr	0.01 ± 0.01		0.02 ± 0.03	
KS UMa	0.05 ± 0.05		0.03 ± 0.08	

Results are listed in Table 2 and shown in Fig.4. Before discussing them we must make few comments. In the case of low inclination systems with no orbital elements the zero point of ϕ_{orb} and, consequently, of ϕ_b are arbitrary. The orbital

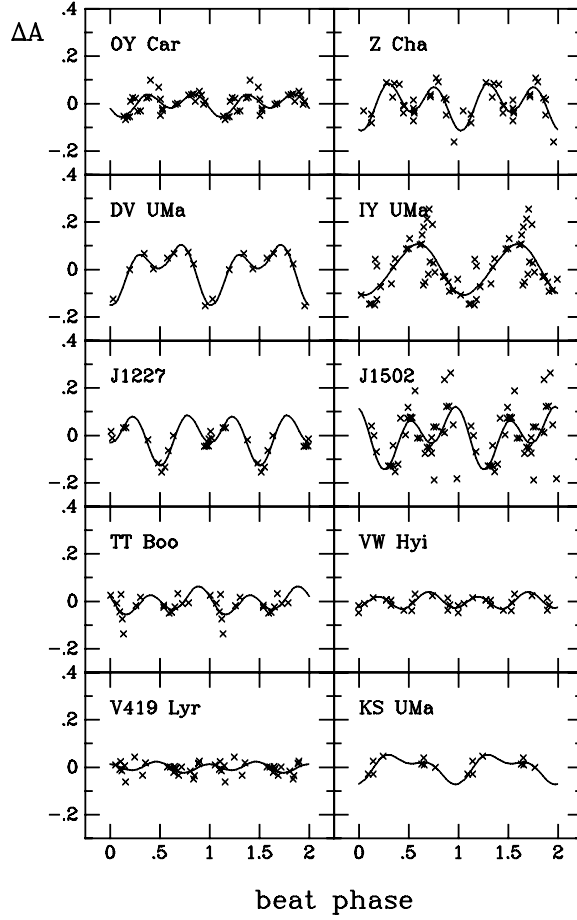


Fig. 4. Residual superhump amplitudes vs. beat phase for 6 high inclination and 4 low inclination systems. Zero points of ϕ_b for TT Boo, VW Hyi, V419 Lyr and KS UMa are arbitrary. Solid lines are cosine and double cosine curves with parameters obtained from solutions using Eq.(10) and listed in Table 2. See text for details.

period of VW Hyi was taken from Vogt (1974), while for three other systems it was calculated from P_{sh} using formula given by Menninkent et al. (1999).

The expected "single- ϕ_b " modulation is present in all high inclination systems (although in the case of OY Car it is barely significant). The mean value of A_1 for those six systems is: $\langle A_1 \rangle = 0.06$ (with *r.m.s.* dispersion of individual values being $\sigma = 0.03$), while in the case of the four low inclination systems it is only $\langle A_1 \rangle = 0.02$ (with $\sigma = 0.02$). The mean value of $\phi_{b,1}^{max}$ for 5 high inclination systems – excluding the deviating value for J1227+5139 – is $\langle \phi_{b,1}^{max} \rangle = 0.62$ (with $\sigma = 0.06$) or – including J1227+5139 – $\langle \phi_{b,1}^{max} \rangle = 0.68$ (with $\sigma = 0.08$). In either case this is consistent with $\langle \phi_b^{max} \rangle = 0.65 \pm 0.02$ obtained from disk luminosity modulation (see above).

Turning to the "double- ϕ_b " modulation we find that it is present in five high inclination systems, the only exception being IY UMa. The mean value of A_2 – including IY UMa – is $\langle A_2 \rangle = 0.06$ ($\sigma = 0.03$) to be compared with only $\langle A_2 \rangle = 0.03$ ($\sigma = 0.02$) for low inclination systems. The mean value of $\phi_{b,2}^{max}$ – excluding IY UMa – is $\langle \phi_{b,2}^{max} \rangle = 0.33$ (with $\sigma = 0.09$) or – excluding also the deviating value for J1502+3334 – $\langle \phi_{b,2}^{max} \rangle = 0.29$ (with $\sigma = 0.04$). We adopt: $\langle \phi_{b,2}^{max} \rangle = 0.30$. It may be added that the value obtained earlier for U Gem (Smak 2006), namely $\phi_{b,2}^{max} \approx 0.15 \pm 0.13$ is – within errors – practically the same.

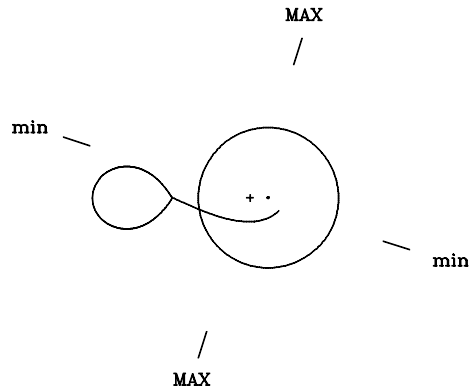


Fig. 5. Schematic model of a cataclysmic binary with $q = 0.15$ showing the secondary, the disk (for simplicity shown circular), and the stream trajectory. The position of the center of mass is marked with a cross. Phases of highest and lowest superhump amplitudes are marked with "MAX" and "min".

The presence of the "double- ϕ_b " modulation and, in particular, the value of $\langle \phi_{b,2}^{max} \rangle$ provide an important clue concerning the location of the superhump light source. Fig.5 presents schematic view of a system with $q = 0.15$ (typical for systems considered here). Shown there are the two phases of the highest superhump amplitudes: $\phi_b^{max} = \phi_{orb}^{max} = 0.30$ and 0.80 and two other phases corresponding to the lowest amplitudes: $\phi_b^{min} = \phi_{orb}^{min} = 0.05$ and 0.55 . The conclusion is obvious: the orientation of the superhump light source is correlated with the direction of the stream. More specifically: the maximum superhump amplitude occurs when the line of sight is perpendicular to the stream (including its part overflowing the disk), while the minimum amplitude – when the line of sight is parallel to the stream.

4. Superhump Amplitudes in Permanent Superhumpers

Table 3 contains representative sample of ten permanent superhumpers including data on their superhump amplitudes. Regretfully, there are only two eclipsing systems with moderately high inclination. Therefore not much weight can be given to the fact that their amplitudes are practically the same as at lower inclinations.

Table 3
Amplitudes of Superhumps
Nova-Like Permanent Superhumpers

Star	i	A(mag)	Data source
V603 Aql	13	0.12	Patterson et al. (1993) Table 1
TT Ari		0.15	Skillman et al. (1998) Fig.2
V592 Cas		0.15	Taylor et al. (1998) Fig.1
TV Col		0.08	Retter et al. (2003) Fig. 4 Hellier (1993)
BB Dor		0.08	Patterson et al. (2005) Fig.7
V795 Her		0.22	Patterson and Skillman (1994)
BK Lyn		0.06	Skillman and Patterson (1993) Fig.6
MV Lyr	12	0.11	Borisov (1992) Fig.4
V348 Pup	81.1	0.11	Rolfe et al.(2000) Fig.6
DW UMa	82.0	0.13	Stanishev et al. (2004) Fig.4 Patterson et al. (2002) Fig.15

The mean superhump amplitude for objects listed in Table 3 is $\langle A \rangle = 0.12$ mag. This is much lower than the maximum amplitudes observed during superoutbursts, comparable to the amplitudes observed near the end of a superoutburst. Two possible explanations of this difference could be proposed. The lower superhump amplitudes in permanent superhumpers could be due to a higher mass transfer rate and higher luminosity of the disk. On the other hand, it could be speculated that the higher maximum superhump amplitudes in dwarf novae are due to a sudden enhancement of the mass transfer rate at the beginning of a superoutburst.

5. The Nature of Superhumps

5.1. The Tidal-Resonance Model

The commonly accepted tidal-resonance model, first proposed by Whitehurst (1988) and Hirose and Osaki (1990), explains superhumps as being due to tidal effects in the outer parts of accretion disks leading – via the 3:1 resonance – to the

formation of an eccentric outer ring undergoing apsidal motion. This model and, in particular, the results of numerous 2D and 3D SPH simulations (cf. Smith et al. 2007 and references therein) reproduce the observed superhump periods and correlations of the superhump period excess with the orbital period and the mass-ratio. This suggests that the basic "clock" which defines the superhump periods is probably provided by the apsidal motion (but see point (1) below).

On the other hand, however, the tidal-resonance model fails to explain all other important facts:

(1) The 3:1 resonance, which is the crucial ingredient of the tidal-resonance model, can occur only in systems with mass ratios $q = M_2/M_1$ smaller than $q_{crit} = 0.25$ (cf. Whitehurst 1988, Osaki 2005 and references therein; see also Smak 2006 for a critical review of attempts to increase q_{crit} up to 0.33). The condition $q < q_{crit}$ is fulfilled by the short period dwarf novae of the SU UMa type. There are, however, other systems with mass ratios higher than q_{crit} which also show superhumps. Examples: dwarf novae U Gem with $q = 0.36 \pm 0.02$ (Smak 2001), and TU Men with $q \approx 0.5 \pm 0.2$ or $q > 0.41 \pm 0.08$ (Smak 2006), and the growing number of permanent superhumpers with longer orbital periods indicating much higher mass ratios; among them: MV Lyr with $q = 0.43^{+0.19}_{-0.13}$ (Skillman et al. 1995), DW UMa with $q = 0.39 \pm 0.12$ (Araujo-Betancor et al. 2003), BH Lyn with $q = 0.45^{+0.15}_{-0.10}$ (Hoard and Szkody 1997), and TV Col with $q = 0.62 - 0.93$ (Hellier 1993) or $q = 0.92 \pm 0.12$ (Retter et al. 2003).

(2) Numerical 2D and 3D SPH simulations produce "superhumps" with visual amplitudes which are smaller than $A = 0.10$ (from 2D models), or as small as $A = 0.03 - 0.04$ (from 3D models) (see Smak 2009a and references therein). They are by factor 4 – 10 smaller than $\langle A_n \rangle = 0.34 \pm 0.02$ obtained from observations in Section 3.2.

(3) The dependence of superhump amplitudes on the orbital inclination (Section 3.2) eliminates all models which locate the source of superhumps within the disk.

(4) The presence and characteristics of obscuration effects which affect superhump amplitudes in systems with high orbital inclinations (Sections 3.2 and 3.3) imply also that the superhump source is not located within the disk but extends sufficiently high above its surface to avoid full obscuration.

(5) The presence of the "double- ϕ_b " modulation of superhump amplitudes related to the orientation of the stream (Section 3.3) finds no explanation within the tidal-resonance model.

5.2. *An Alternative Interpretation of Superhumps*

Using evidence available earlier it was proposed (Smak 2009b) that superhumps are due to periodically modulated dissipation of the kinetic energy of the

stream, the essential ingredients of this interpretation being as follows:

(1) The outer parts of the disk have a non-axisymmetric structure, involving the azimuthal dependence of their vertical thickness, rotating – in the inertial frame – with P_b .

(2) This causes the irradiation of the secondary component to be modulated with P_{irr} (related to P_b and P_{orb}), resulting in periodic variations of the mass transfer rate with $P_{sh} \approx P_{irr}$.

(3) Around superhump maximum the stream overflows the surface of the disk and – unlike in the case of the "standard" hot spot – its energy is dissipated along its trajectory above (and below) the disk.

(4) The periodically variable dissipation of the kinetic energy of the stream is observed in the form of superhumps.

Results presented in this paper provide further arguments in favor of this interpretation. In particular:

(1) The presence and characteristics of obscuration effects which affect superhump amplitudes in systems with high orbital inclinations (Sections 3.2 and 3.3) imply that the superhump light source is indeed located above the surface of the disk.

(2) The "double- ϕ_b " modulation of the superhump amplitudes (Section 3.3) implies that the orientation of the superhump light source is – as could be expected – correlated with the direction of the stream. In particular, when the line of sight is perpendicular to the stream trajectory, the superhump must be brighter due to larger projected surface area of the overflowing parts of the stream.

6. Conclusions

The new results concerning superhump amplitudes, their dependence on orbital inclination, and their modulation with the beat phase, presented in this paper, provide further arguments against the commonly accepted tidal-resonance model for superhumps. At the same time they support the alternative interpretation of superhumps involving the periodically modulated dissipation of the kinetic energy of the stream.

REFERENCES

- Araujo-Betancor, S. et al. 2003, *ApJ*, **583**, 437.
 Borisov, G.V. 1992, *A&A*, **261**, 154.
 Boyd, D., Oksanen, A., Henden, A. 2006, *J.Br.Astron.Assoc.*, **116**, 187.
 Haefner, R., Schoembs, R., Vogt, N. 1979, *A&A*, **77**, 7.

- Harvey, D.A., Patterson, J. 1995, *PASP*, **107**, 1055.
- Harvey, D.A., Skillman, D.R., Patterson, J., Ringwald, F.A. 1995, *PASP*, **107**, 551.
- Hellier, C. 1993, *MNRAS*, **264**, 132.
- Hellier, C. 2001, *Cataclysmic Variable Stars* (Springer) .
- Hirose, M., Osaki, Y. 1990, *Publ.Astr.Soc.Japan*, **42**, 135.
- Hoard, D.W., Szkody, P. 1997, *ApJ*, **481**, 433.
- Kato, T. et. al. 2003, *MNRAS*, **339**, 861.
- Kato, T. et. al. 2009, *Publ.Astr.Soc.Japan*, **61**, S395.
- Kiyota, S., Kato, T. 1998, *Inf.Bull.Var.Stars*, No.4664.
- Krzemiński, W., Vogt, N. 1985, *A&A*, **144**, 124.
- Menninckent, R.E., Matsumoto, K., Arenas, J. 1999, *A&A*, **348**, 466.
- Olech, A. 1997, *Acta Astron.*, **47**, 281.
- Olech, A. 2003, *Acta Astron.*, **53**, 85.
- Olech, A., Schwarzenberg-Czerny, A., Kędzierski, P., Złoczewski, K., Mularczyk, K., Wiśniewski, M. 2003, *Acta Astron.*, **53**, 175.
- Olech, A., Złoczewski, K., Mularczyk, K., Kędzierski, P., Wiśniewski, M., Stachowski, G. 2004a, *Acta Astron.*, **54**, 57.
- Olech, A., Cook, L.M., Złoczewski, K., Mularczyk, K., Kędzierski, P., Udalski, A., Wiśniewski, M. 2004b, *Acta Astron.*, **54**, 233.
- Olech, A., Złoczewski, K., Cook, L.M., Mularczyk, K., Kędzierski, P., Wiśniewski, M. 2005, *Acta Astron.*, **55**, 237.
- Osaki, Y. 2005, *Proc.Japan Academy, Ser.B*, **81**, 291.
- Patterson, J. 1999, *Disk Instabilities in Close Binary Systems*, eds. S.Mineshige and J.C.Wheeler (Tokyo: Universal Academy Press) , 61.
- Patterson, J., Thomas, G., Skillman, D.R., Diaz, M. 1993, *ApJS*, **86**, 235.
- Patterson, J., Skillman, D.R. 1994, *PASP*, **106**, 1141.
- Patterson, J., Jablonsky, F., Koen, C., O'Donoghue, D., Skillman, D.R. 1995, *PASP*, **107**, 1183.
- Patterson, J. et al. 1998, *PASP*, **110**, 1290.
- Patterson, J., Kemp, J., Jensen, L., Vanmunster, T., Skillman, D.R., Martin, B., Fried, R., Thorstensen, J.R. 2000a, *PASP*, **112**, 1567.
- Patterson, J., Vanmunster, T., Skillman, D.R., Jensen, L., Stull, J., Martin, B., Cook, L.M., Kemp, J., Knigge, C. 2000b, *PASP*, **112**, 1584.
- Patterson, J. et al. 2002, *PASP*, **114**, 1364.
- Patterson, J. et al. 2005, *PASP*, **117**, 1204.
- Retter, A., Hellier, C., Augustejn, T., Naylor, T., Bedding, T.R., Bembrick, C., McCormick, J., Velthuis, F. 2003, *MNRAS*, **340**, 679.
- Ritter, H., Kolb, U. 2003, *A&A*, **404**, 301. (update RKcat. 7.14, 2010)
- Rolfé, D.J., Haswell, C.A., Patterson, J. 2000, *MNRAS*, **317**, 759.
- Rutkowski, A., Olech, A., Mularczyk, K., Boyd, D., Koff, R., Wiśniewski, M. 2007, *Acta Astron.*, **57**, 267.
- Rutkowski, A., Olech, A., Wiśniewski, M., Pietrukowicz, P., Pala, J., Poleski, R. 2009, *A&A*, **497**, 437.
- Schoembs, R. 1986, *A&A*, **158**, 233.
- Semeniuk, I. 1980, *A&AS*, **39**, 29.
- Shears, J., Brady, S., Foote, J., Starkey, D., Vanmunster, T. 2008, *J.Br.Astron.Assoc.*, **118**, 288.
- Shears, J. et al. 2010, arXiv, 1005.3219.
- Skillman, D.R., Patterson, J. 1993, *ApJ*, **417**, 298.
- Skillman, D.R., Patterson, J., Thorstensen, J.R. 1995, *PASP*, **107**, 545.
- Skillman, D.R. et al. 1998, *ApJ*, **503**, L67.
- Smak, J. 2001, *Acta Astron.*, **51**, 279.
- Smak, J. 2006, *Acta Astron.*, **56**, 365.
- Smak, J. 2009a, *Acta Astron.*, **59**, 103.

- Smak, J. 2009b, *Acta Astron.*, **59**, 121.
- Smak, J., Waagen, E.O. 2004, *Acta Astron.*, **54**, 433.
- Smith, A.J., Haswell, C.A., Murray, J.R., Truss, M.R., Foulkes, S.B. 2007, *MNRAS*, **378**, 785.
- Soejima, Y. et al. 2009, *Publ.Astr.Soc.Japan*, **61**, 659.
- Stanishev, V., Kraicheva, Z., Boffin, H.M.J., Genkov, V., Papadaki, C., Carpano, S. 2004, *A&A*, **416**, 1057.
- Still, M., Howell, S.B., Wood, M.A., Cannizzo, J.K., Smale, A.P. 2010, *ApJ*, **717**, L113.
- Taylor, C.J., Thorstensen, J.R., Patterson, J., Fried, R.E., Vanmunster, T., Harvey, D.A., Skillman, D.R., Jensen, L., Shugarov, S. 1998, *PASP*, **110**, 1148.
- Uemura, M. et al. 2004, *Publ.Astr.Soc.Japan*, **56**, 141.
- Vogt, N. 1974, *A&A*, **36**, 369.
- Warner, B. 1975, *MNRAS*, **170**, 219.
- Warner, B. 1985, *Interacting Binaries*, eds. P.P.Eggleton, and J.E.Pringle (Reidel) , 367.
- Warner, B. 1995, *Cataclysmic Variable Stars*. (Cambridge University Press).
- Warner, B., O'Donoghue, D. 1988, *MNRAS*, **233**, 705.
- Whitehurst, R. 1988, *MNRAS*, **232**, 35.